

EM duality and Quasi-normal modes from higher derivatives with homogeneous disorder

Guoyang Fu ^{1*} and Jian-Pin Wu ^{2†}

¹ *Department of Physics,
School of Mathematics and Physics,
Bohai University,
Jinzhou 121013, China*

² *Center for Gravitation and Cosmology,
College of Physical Science and Technology,
Yangzhou University,
Yangzhou 225009, China*

Abstract

We study the electromagnetic (EM) duality from 6 derivative theory with homogeneous disorder. We find that with the change of the sign of the coupling parameter γ_1 of the 6 derivative theory, the particle-vortex duality with homogeneous disorder holds more well than that without homogeneous disorder. The properties of quasinormal modes (QNMs) of this system are also explored. Similarly, for large γ_1 , with the change of the sign of γ_1 , the correspondence between the low frequency poles of the original theory and the ones of its dual theory, which is strongly violated in the absence of homogeneous disorder, holds well. Some new branch cuts of QNMs emerge for some system parameters.

*FuguoyangEDU@163.com

†jianpinwu@yzu.edu.cn

I. INTRODUCTION

Holographic quantum critical (QC) dynamics at zero density has been deeply explored [1–12]. It provides a powerful tool to study strongly coupled systems without quasi-particles descriptions. By studying the transports, in particular the optical conductivity, from a probe Maxwell field coupled to the Weyl tensor $C_{\mu\nu\rho\sigma}$ on top of the 4 dimensional Schwarzschild-AdS (SS-AdS) black brane background¹ [1–9], they observe a non-trivial frequency dependent conductivity attributing to the introduction of Weyl tensor, which breaks the electromagnetic (EM) duality. It exhibits a peak, which resembles the particle response and we refer as the Damle-Sachdev (DS) peak² [14], or a dip, which is similar with the behavior of the vortex response. Such behavior is analogous to the one in the superfluid-insulator quantum critical point (QCP) [1–3]. In addition, the DC conductivity has a bound, which can not arrive at zero in the allowed region of coupling parameter. When higher derivative (HD) terms are introduced, an arbitrarily sharp DS peak can be observed at low frequency in the optical conductivity depending on the coupling parameters, and the bound of conductivity in 4 derivative theory is violated such that a zero DC conductivity can be obtained at specific parameter [8]. In particular, its behavior is quite closely analogous to that of the $O(N)$ superfluid-insulator model in the limit of large- N [14]. Another progress is the construction of neutral scalar hair black brane by coupling Weyl tensor with neutral scalar field, which provides a framework to describe QC dynamics and one away from QCP [11–13].

Also, we can introduce a mechanism of microscopic translational symmetry broken, for example [15–25], which leads to the momentum dissipation of the dual field theory and is also referred as homogeneous disorder, into the holographic QC system [1–12], such that we can study the effects from homogeneous disorder on these systems [26–29]. We find that for 4 derivative theory studied in [26], the homogeneous disorder drives the incoherent metallic state with DS peak into the one with a dip for $\gamma > 0$ and an opposite scenario is found for $\gamma < 0$. But for the 6 derivative theory explored in [27], the homogeneous disorder cannot make the peak (gap) transform into its contrary. Another interesting phenomena is that

¹ Since the Maxwell field is the 1 derivative term and the Weyl tensor is the 2 derivative term, the coupling term as $C_{\mu\nu\rho\sigma}F^{\mu\nu}F^{\rho\sigma}$ is the 4 derivative term. Therefore, we also refer to this theory as 4 derivative theory.

² Since the peak results from the particle-hole symmetry at zero charge density but not the breaking of translation symmetry, we refer as DS peak instead of Drude peak.

for 4 derivative theory there is a specific value of $\hat{\alpha} = 2/\sqrt{3}$, for which the particle-vortex duality, corresponding to EM duality in bulk, almost exactly holds with the change of the sign of γ [26].

On the other hand, to study the holographic QC dynamics, a good method we can use is the quasinormal modes (QNMs) of a gravitational theory on the bulk AdS spacetime. Recently, the structure of the QNMs of 4/6 derivative theory over SS-AdS has been explored [5, 8]. In particular, the particle-vortex duality has also been discussed. Further, when the homogeneous disorder in 4 derivative theory is introduced, more rich pole structures are exhibited [29]. In this paper, we shall study the EM duality and the QNMs of 6 derivative theory with homogeneous disorder. Our paper is organized as what follows. In Section II, we present a brief introduction on the 6 derivative theory with homogeneous disorder. EM duality is discussed in Section III. In Section IV, we study the properties of the QNMs. A brief discussion is presented in Section V. In Appendix A, we also give a brief discussion on the instabilities of gauge mode by the QNMs.

II. HOLOGRAPHIC SETUP

We consider the following neutral Einstein-axions (EA) theory [15],

$$S_0 = \int d^4x \sqrt{-g} \left(R + \frac{6}{L^2} - \frac{1}{2} \sum_{I=x,y} (\partial\phi_I)^2 \right). \quad (1)$$

In the above action, we have introduced a pair of spatial linear dependent axionic fields, $\phi_I = \alpha x_I$ with $I = x, y$ and α being a constant, which are responsible for dissipating the momentum of the dual boundary field. L is the radius of the AdS spacetimes.

From the EA action (1), we have a neutral black brane solution [15]

$$ds^2 = \frac{L^2}{u^2} \left(-f(u)dt^2 + \frac{1}{f(u)}du^2 + dx^2 + dy^2 \right), \quad (2)$$

where

$$f(u) = (1-u)p(u), \quad p(u) = \frac{\sqrt{1+6\hat{\alpha}^2} - 2\hat{\alpha}^2 - 1}{\hat{\alpha}^2} u^2 + u + 1. \quad (3)$$

The AdS boundary is at $u = 0$ and the horizon locates at $u = 1$. $\hat{\alpha} \equiv \alpha/4\pi T$ with the Hawking temperature $T = p(1)/4\pi$. Since the translational symmetry breaks, the momentum dissipates. But the geometry is homogeneous and so we refer to this mechanism

as homogeneous disorder and $\hat{\alpha}$ denotes the strength of disorder. Therefore, the background describes a specific thermal excited state with homogeneous disorder.

Over this background, we study the following HD action for gauge field coupling with Weyl tensor

$$S_A = \int d^4x \sqrt{-g} \left(-\frac{1}{8g_F^2} F_{\mu\nu} X^{\mu\nu\rho\sigma} F_{\rho\sigma} \right), \quad (4)$$

where the tensor X is an infinite family of HD terms [8]

$$\begin{aligned} X_{\mu\nu}{}^{\rho\sigma} = & I_{\mu\nu}{}^{\rho\sigma} - 8\gamma_{1,1} L^2 C_{\mu\nu}{}^{\rho\sigma} - 4L^4 \gamma_{2,1} C^2 I_{\mu\nu}{}^{\rho\sigma} - 8L^4 \gamma_{2,2} C_{\mu\nu}{}^{\alpha\beta} C_{\alpha\beta}{}^{\rho\sigma} \\ & - 4L^6 \gamma_{3,1} C^3 I_{\mu\nu}{}^{\rho\sigma} - 8L^6 \gamma_{3,2} C^2 C_{\mu\nu}{}^{\rho\sigma} - 8L^6 \gamma_{3,3} C_{\mu\nu}{}^{\alpha_1\beta_1} C_{\alpha_1\beta_1}{}^{\alpha_2\beta_2} C_{\alpha_2\beta_2}{}^{\rho\sigma} + \dots \end{aligned} \quad (5)$$

Note that $I_{\mu\nu}{}^{\rho\sigma} = \delta_\mu{}^\rho \delta_\nu{}^\sigma - \delta_\mu{}^\sigma \delta_\nu{}^\rho$ is an identity matrix and $C^n = C_{\mu\nu}{}^{\alpha_1\beta_1} C_{\alpha_1\beta_1}{}^{\alpha_2\beta_2} \dots C_{\alpha_{n-1}\beta_{n-1}}{}^{\mu\nu}$. In the above equations, the factor of L is introduced such that the coupling parameters g_F and $\gamma_{i,j}$ are dimensionless. But for later convenience, we work in units where $L = 1$ in what follows and set $g_F = 1$ in the numerical calculation. When $X_{\mu\nu}{}^{\rho\sigma} = I_{\mu\nu}{}^{\rho\sigma}$, the theory reduces to the standard Maxwell theory. For convenience, we denote $\gamma_{1,1} = \gamma$ and $\gamma_{2,i} = \gamma_i (i = 1, 2)$. In this paper, our main focus is the 6 derivative terms, i.e., γ_1 and γ_2 terms. At the same time, since the effect of both γ_1 and γ_2 terms is similar, we only turn on γ_1 term through this paper. Note that when other parameters are turned off, γ_1 is confined in the region $\gamma_1 \leq 1/48$ over SS-AdS black brane background³ [8]. And then, from the action (4), we can write down the equation of motion (EOM) as,

$$\nabla_\nu (X^{\mu\nu\rho\sigma} F_{\rho\sigma}) = 0. \quad (6)$$

As [1], the dual EM theory of (4) can be constructed, which is

$$S_B = \int d^4x \sqrt{-g} \left(-\frac{1}{8\hat{g}_F} G_{\mu\nu} \hat{X}^{\mu\nu\rho\sigma} G_{\rho\sigma} \right). \quad (7)$$

$G_{\mu\nu} \equiv \partial_\mu B_\nu - \partial_\nu B_\mu$ is the dual field strength and \hat{g}_F is the coupling constant, which relates g_F as $\hat{g}_F^2 \equiv 1/g_F^2$. \hat{X} is the dual tensor, which satisfies

$$\hat{X}_{\mu\nu}{}^{\rho\sigma} = -\frac{1}{4} \varepsilon_{\mu\nu}{}^{\alpha\beta} (X^{-1})_{\alpha\beta}{}^{\gamma\lambda} \varepsilon_{\gamma\lambda}{}^{\rho\sigma}, \quad \frac{1}{2} (X^{-1})_{\mu\nu}{}^{\rho\sigma} X_{\rho\sigma}{}^{\alpha\beta} \equiv I_{\mu\nu}{}^{\alpha\beta}. \quad (8)$$

³ In [27], they also study the instabilities of the gauge mode and the causality in CFT, in addition to the constraint from $\text{Re}\sigma(\omega) \geq 0$, they confirm that the constraint $\gamma_1 \leq 1/48$ also holds over EA-AdS geometry.

And then, the EOM of the dual theory (7) can be wrote down as

$$\nabla_\nu(\widehat{X}^{\mu\nu\rho\sigma}G_{\rho\sigma}) = 0. \quad (9)$$

For the four dimensional standard Maxwell theory, $\widehat{X}_{\mu\nu}^{\rho\sigma} = I_{\mu\nu}^{\rho\sigma}$. At this moment, both the theories (4) and (7) are identical and so the standard Maxwell theory is self-dual. Once the HD terms are introduced, such self-duality is broke. However, if γ_1 is small, we have

$$(X^{-1})_{\mu\nu}^{\rho\sigma} = I_{\mu\nu}^{\rho\sigma} + 4\gamma_1 C^2 I_{\mu\nu}^{\rho\sigma} + \mathcal{O}(\gamma_1^2), \quad (10)$$

$$\widehat{X}_{\mu\nu}^{\rho\sigma} = (X^{-1})_{\mu\nu}^{\rho\sigma} + \mathcal{O}(\gamma_1^2). \quad (11)$$

It indicates that for small γ_1 , there is an approximate duality between both theories (4) and (7) with the change of the sign of γ_1 .

III. CONDUCTIVITY AND EM DUALITY

Turning on the perturbation $A_y(t, u) \sim e^{-i\omega t} A_y(u)$, we can write down the EOM of gauge field [1, 26, 27]

$$A_y'' + \left(\frac{f'}{f} + \frac{X_6'}{X_6}\right)A_y' + \frac{\mathbf{p}^2\hat{\omega}^2}{f^2} \frac{X_2}{X_6} A_y = 0, \quad (12)$$

where X_i , $i = 1, \dots, 6$, are the components of X_A^B defined as $X_A^B = \{X_1(u), X_2(u), X_3(u), X_4(u), X_5(u), X_6(u)\}$, with $A, B \in \{tx, ty, tu, xy, xu, yu\}$. Due to the isotropy of background, $X_1(u) = X_2(u)$ and $X_5(u) = X_6(u)$. In addition, we have defined the dimensionless frequency in the above equation $\hat{\omega} \equiv \frac{\omega}{4\pi T} = \frac{\omega}{\mathbf{p}}$, with $\mathbf{p} \equiv p(1) = 4\pi T$. Letting $X_i \rightarrow \widehat{X}_i = 1/X_i$, we can obtain the dual EOM. Solving the EOM (12) or the dual EOM with ingoing boundary condition at the horizon, we can read off the conductivity in terms of

$$\sigma(\hat{\omega}) = \frac{\partial_u A_y(u, \hat{\omega})}{i\hat{\omega}\mathbf{p}A_y(u, \hat{\omega})}. \quad (13)$$

It has been illustrated in the last section that for very small γ_1 , there is an approximate duality between both the original EM theory and its dual theory with the change of the sign of γ_1 as that for 4 derivative theory [1, 26]. At the same time, there is an inverse relation for the conductivity of the original theory and its dual theory⁴[1, 5]

$$\sigma_*(\hat{\omega}; \hat{\alpha}, \gamma_1) = \frac{1}{\sigma(\hat{\omega}; \hat{\alpha}, \gamma_1)}, \quad (14)$$

⁴ This relation has been proved in [1, 5]. Also it has been derived for a specific class of CFTs in [30].

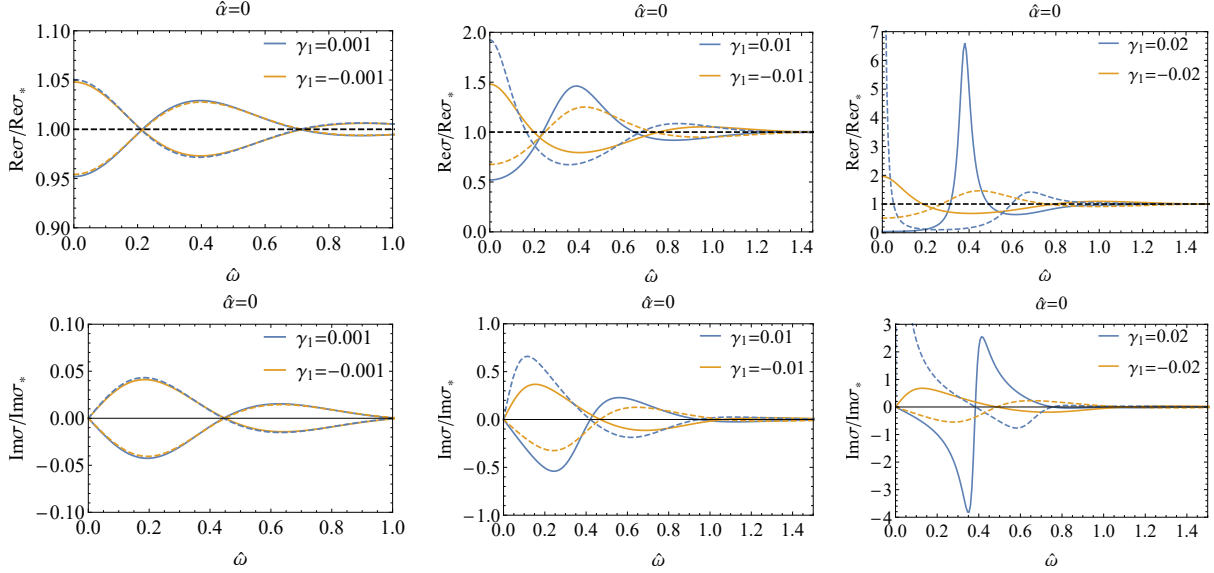


FIG. 1: The real part (the plot above) and the imaginary part (the plot below) of the optical conductivity as the function of $\hat{\omega}$ for $\hat{\alpha} = 0$ and various values of γ_1 . The solid curves are the conductivity σ of the original EM theory (4) and the dashed curves display the conductivity σ_* of the EM dual theory (7).

where σ_* is the conductivity of the dual theory. Therefore, for small γ_1 , we conclude that [26]

$$\sigma_*(\hat{\omega}; \hat{\alpha}, \gamma_1) \approx \sigma(\hat{\omega}; \hat{\alpha}, -\gamma_1), \quad |\gamma_1| \ll 1. \quad (15)$$

It indicates that the dual optical conductivity is approximately equal to its original one with the change of the sign of γ_1 . For 4 derivative theory, it has been studied and found that the conductivity of the dual EM theory is not precisely equal to that of its original theory with the change of the sign of γ [1]. But when the homogeneous disorder is introduced, we find that this relation holds more well for a specific value of $\hat{\alpha} = 2/\sqrt{3}$ than other value of $\hat{\alpha}$. Here, we shall study the EM duality from 6 derivative theory.

FIG.1 exhibits the optical conductivity as the function of $\hat{\omega}$ for $\hat{\alpha} = 0$ and various values of γ_1 . We find that for small $|\gamma_1|$ ($|\gamma_1| = 0.001$), with the change of the sign of γ_1 , the relation (15) holds very well. With the increase of $|\gamma_1|$, the relation (15) violates. In particular for $\gamma_1 = 0.02$, the real part of the conductivity at low frequency is a pseudogap-like behavior. Correspondingly, its dual conductivity $\text{Re}\sigma_*$ at low frequency becomes sharper, which is Drude-like. But for $\gamma_1 = -0.02$, the real parts of the conductivity of the original theory

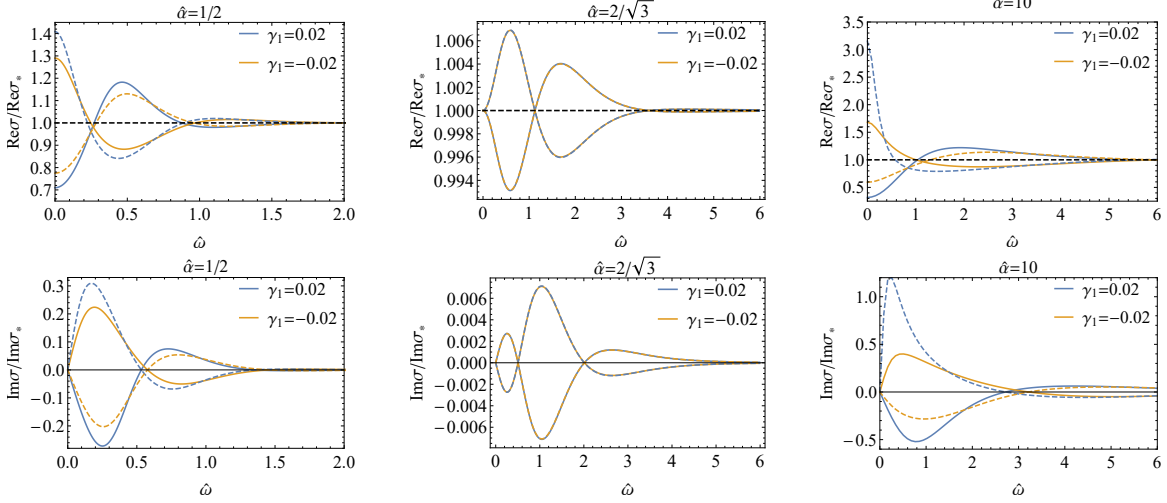


FIG. 2: The real part (the plot above) and the imaginary part (the plot below) of the optical conductivity as the function of $\hat{\omega}$ for $|\gamma_1| = 0.02$ and various values of $\hat{\alpha}$. The solid curves are the conductivity σ of the original EM theory (4) and the dashed curves display the conductivity σ_* of the EM dual theory (7).

and its dual one at low frequency are only peak and dip, respectively. At this moment, the relation (15) is strongly violated.

Next, we explore the EM duality for 6 derivative theory when the homogeneous disorder is introduced. At the first sight, we find that for the specific value of $\hat{\alpha} = 2/\sqrt{3}$, the optical conductivity of the original theory is almost (approximate but not exact) the same as that of the dual one when the sign of γ_1 changes, i.e., the relation (15) holds very well. It is similar to that from 4 derivative theory [26]. For other value of $\hat{\alpha}$, the relation (15) also approximately holds. It seems that the homogeneous disorder make the pseudogap-like of the low frequency conductivity of the original theory becomes small dip, while suppresses the sharp peak of the EM dual theory.

It is hard to obtain an analytical understanding on this phenomenon. But we can follow the method of [26] and attempt to taste kind of analytical similarity between the EOM (12) and its dual one, which can be explicitly wrote down

$$A_y'' + \left(\frac{f'}{f} - \frac{X_6'}{X_6} \right) A_y' + \frac{\mathbf{p}^2}{f^2} \frac{X_6}{X_2} \hat{\omega}^2 A_y = 0. \quad (16)$$

Since $\frac{X_2}{X_6} = \frac{X_6}{X_2}$ for any $\hat{\alpha}$, the difference between Eq.(12) and (16) is in the coefficients of

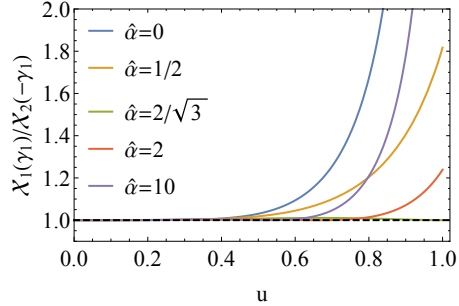


FIG. 3: $\mathcal{X}_1(\gamma_1)/\mathcal{X}_2(-\gamma_1)$ as the function of u with different $\hat{\alpha}$. Here we set $\gamma_1 = 0.02$.

A'_y , which are

$$\mathcal{X}_1(\gamma_1) \equiv \frac{X'_6}{X_6} = \frac{-\frac{16}{3}\gamma_1 u^3 f''(u)^2 - \frac{8}{3}\gamma_1 u^4 f^{(3)}(u) f''(u)}{1 - \frac{4}{3}\gamma_1 u^4 f''(u)^2}, \quad (17)$$

$$\mathcal{X}_2(\gamma_1) \equiv -\frac{X'_6}{X_6} = -\frac{-\frac{16}{3}\gamma_1 u^3 f''(u)^2 - \frac{8}{3}\gamma_1 u^4 f^{(3)}(u) f''(u)}{1 - \frac{4}{3}\gamma_1 u^4 f''(u)^2}. \quad (18)$$

And then, we explicitly plot the ration $\frac{\mathcal{X}_1}{\mathcal{X}_2}\Big|_{\gamma_1=0.02}$ as the function of u with different $\hat{\alpha}$ in FIG.3. For $\hat{\alpha} = 0$, the value of $\frac{\mathcal{X}_1}{\mathcal{X}_2}$ is maximum departure from 1 near the horizon, which indicates a most deviation between (12) and (16). Once the homogeneous disorder is introduced, this deviation become small. Specially, for $\hat{\alpha} = 2/\sqrt{3}$, this value approaches to 1 near the horizon, which implies a most similar between (12) and (16). On the other hand, it is well known that the low frequency behavior of the conductivity is mainly controlled by the near horizon geometry. Therefore, to some extent, the above comparison in the original EOM and its dual one helps us understand the phenomenon shown in FIG.2.

IV. THE PROPERTIES OF QNMS

By definition, QNMs are the poles of the Green's function and are directly related to the conductivity. Summing an increasing number of QNMs and the corresponding residues one should obtain a better and better approximation of the conductivity itself. In this section, we shall study the properties of QNMs of the transverse gauge mode along y direction, i.e., A_y , from 6 derivative term with homogeneous disorder. In particular, we shall also study the particle-vortex duality in the complex frequency panel in the holographic CFT.

It is high efficient to use the pseudospectral methods outlined in [31] to solve the QNM equations and obtain the QNMs. To this end, we shall work in the advanced Eddington-

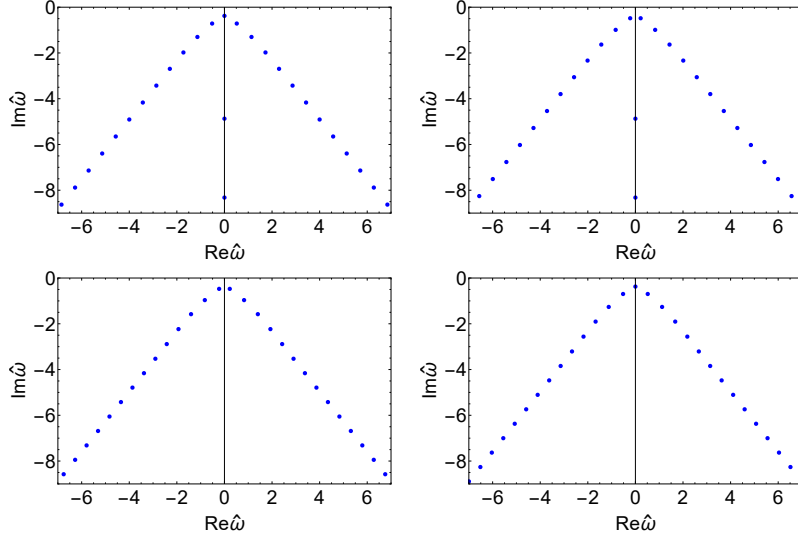


FIG. 4: QNMs (blue spots) of the gauge mode for $|\gamma_1| = 0.001$ (the panels above are for $\gamma_1 = -0.001$ and the ones below for $\gamma_1 = -0.001$) and $\hat{\alpha} = 0$. The left panels are the QNMs of the gauge mode and the right ones are that of the dual gauge mode.

Finkelstein coordinate, which is

$$ds^2 = \frac{1}{u^2} \left(-f(u)dt^2 - 2tdtdu + dx^2 + dy^2 \right). \quad (19)$$

Correspondingly, the EOM (12) can be changed as

$$A'_y \left(\frac{f'}{f} + \frac{2ip\hat{\omega}}{f} + \frac{X'_6}{X_6} \right) + \frac{ip\hat{\omega}A_yX'_2}{fX_6} + A''_y = 0. \quad (20)$$

For the dual theory, the corresponding EOM can be obtained by letting $A_\mu \rightarrow B_\mu$ and $X_i \rightarrow \hat{X}_i = 1/X_i$. Imposing the ingoing boundary at the horizon, we numerically solve Eq. (20) to obtain QNMs.

We first study the case without homogeneous disorder. FIG.4 and 5 show QNMs of the gauge mode with $\hat{\alpha} = 0$ for $|\gamma_1| = 0.001$ and 0.02 , respectively. The left panels are the QNMs of the gauge mode and the right ones are that of the dual gauge mode. We find that for small $|\gamma_1|$, for example, $|\gamma_1| = 0.001$ in FIG.4, the qualitative correspondence between the poles of $\text{Re}\sigma(\hat{\omega}; \gamma_1)$ and the ones of $\text{Re}\sigma_*(\hat{\omega}; -\gamma_1)$ holds well at low frequency. But for the large frequency region, there are some modes emerging at the imaginary frequency axis for negative γ_1 , which results in the violation of the particle-vortex duality with the change of the sign of γ_1 . But with the increase of γ_1 , this correspondence begins to violate in complex frequency panel even in the low frequency region (see FIG.5 for $|\gamma_1| = 0.02$), as that in real

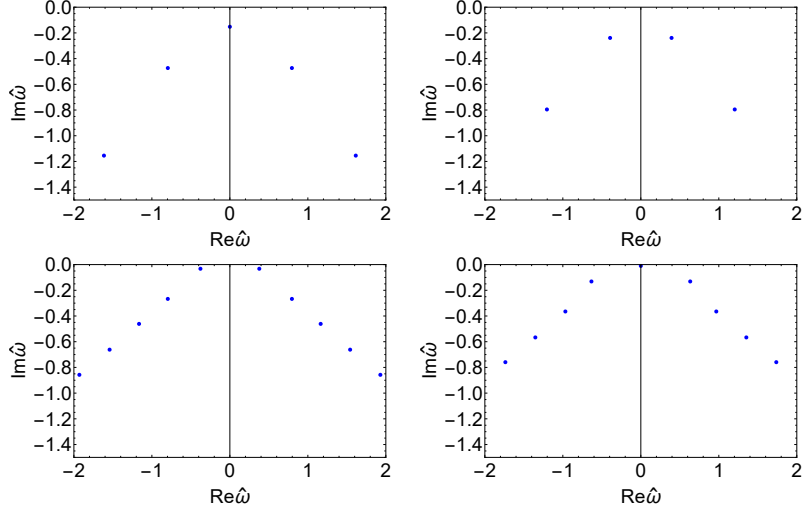


FIG. 5: QNMs (blue spots) of the gauge mode for $|\gamma_1| = 0.02$ (the panels above are for $\gamma_1 = -0.02$ and the ones below for $\gamma_1 = 0.02$) and $\hat{\alpha} = 0$. The left panels are the QNMs of the gauge mode and the right ones are that of the dual gauge mode.

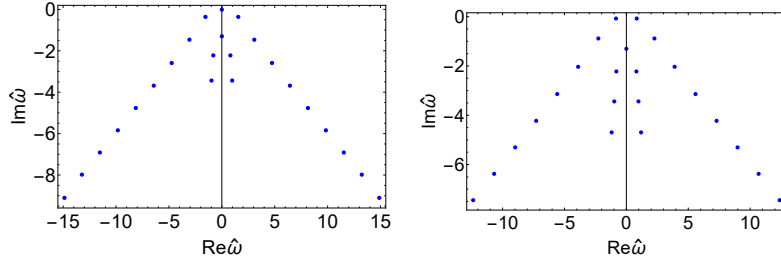


FIG. 6: QNMs (blue spots) of the gauge mode for $\gamma_1 = -1$ and $\hat{\alpha} = 0$. The left panels are the QNMs of the gauge mode and the right ones are that of the dual gauge mode.

frequency axis. We also plot the QNMs for $\gamma_1 = -1$ in FIG.6. We see that another branch cuts, which are closer to the imaginary frequency axis, emerges in the complex frequency panel.

Now we turn to the study of the effects of homogeneous disorder. FIG.7, 8 and 9 show the QNMs with representative $\hat{\alpha}$ for $\gamma = 0.02$, -0.02 and -1 (from left to right) in the complex frequency plane. The panels above are the QNMs of the gauge mode, while the ones below are that of the dual gauge mode. Rich information and insights on the pole structures are exhibited. At the first sight, we find that all the poles are in the lower-half plane (LHP). It indicates that the the gauge mode is stable. Further analysis on stability in terms of QNMs is presented in Appendix A.

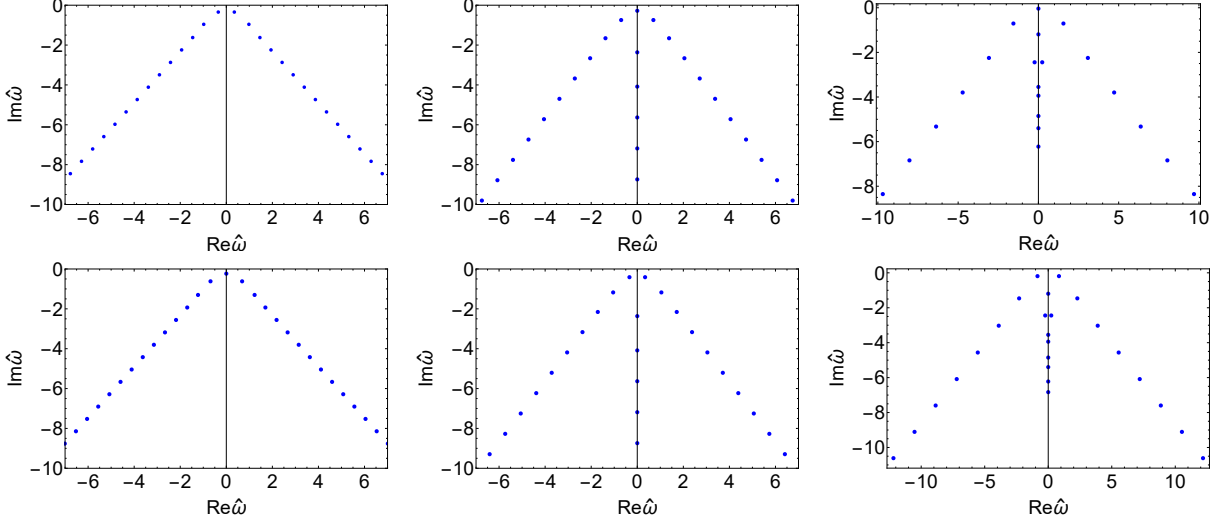


FIG. 7: QNMs (blue spots) of the gauge mode for $\hat{\alpha} = 1/2$. The first, second and third columns are for $\gamma_1 = 0.02$, -0.02 and -1 , respectively. The panels above are for the gauge mode, while the ones below are the dual gauge mode.

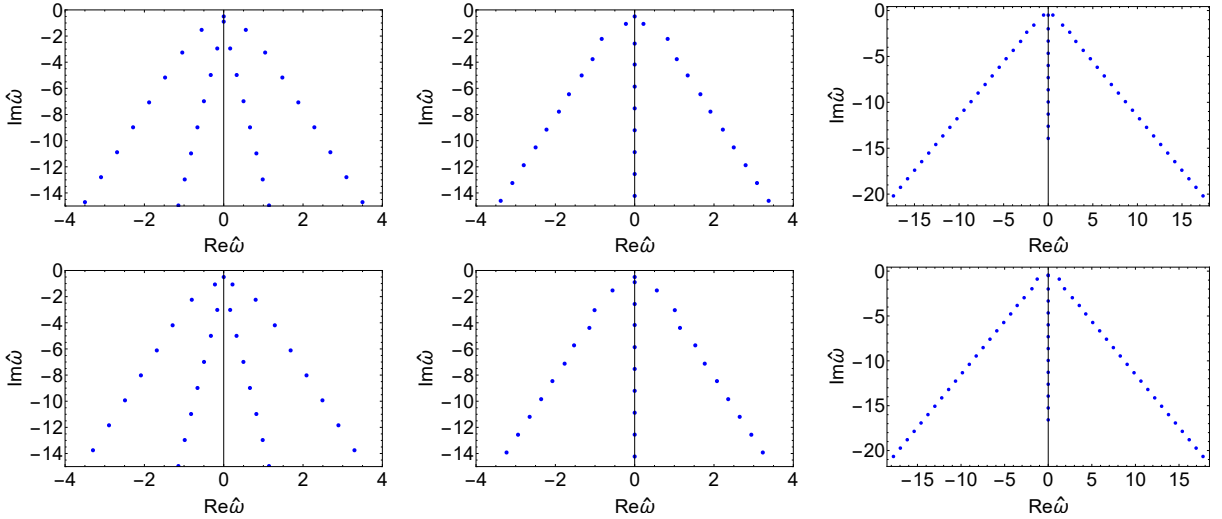


FIG. 8: QNMs (blue spots) of the gauge mode for $\hat{\alpha} = 2/\sqrt{3}$. The first, second and third columns are for $\gamma_1 = 0.02$, -0.02 and -1 , respectively. The panels above are for the gauge mode, while the ones below are the dual gauge mode.

Next, we shall study the main properties of the QNMs when the homogeneous disorder is introduced, in particular, the duality between the poles of $\text{Re}\sigma(\hat{\omega}; \gamma_1)$ and the ones of $\text{Re}\sigma_*(\hat{\omega}; -\gamma_1)$. They are briefly summarized as what follows for $|\gamma_1| = 0.02$.

- For small $\hat{\alpha}$ ($\hat{\alpha} = 1/2$ and $2/\sqrt{3}$), the approximate correspondence between the poles

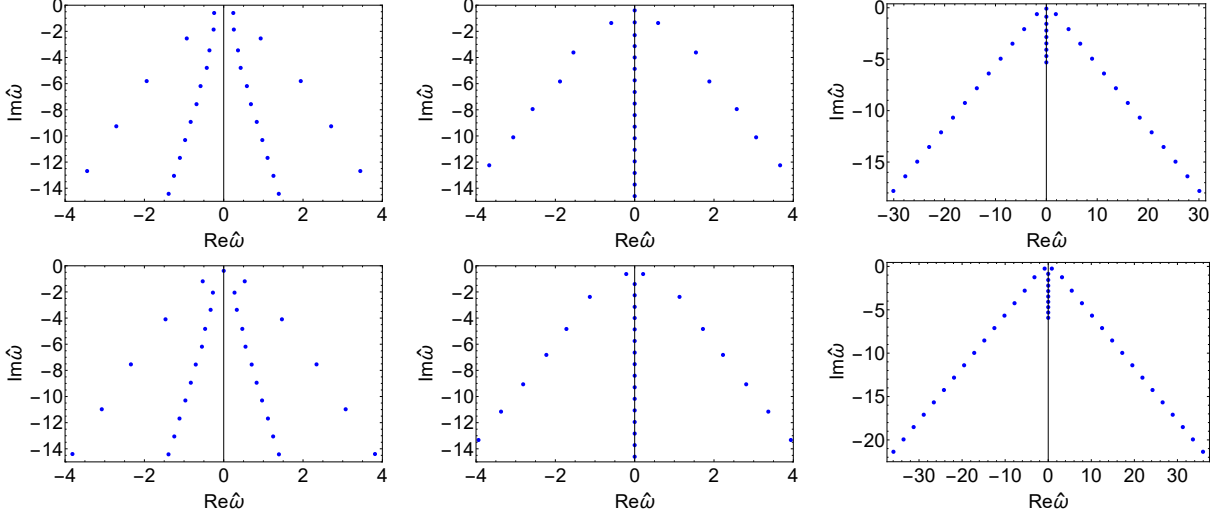


FIG. 9: QNMs (blue spots) of the gauge mode for $\hat{\alpha} = 2$. The first, second and third columns are for $\gamma_1 = 0.02$, -0.02 and -1 , respectively. The panels above are for the gauge mode, while the ones below are the dual gauge mode.

of $\text{Re}\sigma(\hat{\omega}; \gamma_1)$ and the ones of $\text{Re}\sigma_*(\hat{\omega}; -\gamma_1)$ recovers in low frequency region, comparing with that without homogeneous disorder, for which the correspondence is violated. But in the high frequency region, the case becomes different. For $\hat{\alpha} = 1/2$, some modes emerge at the imaginary frequency axis for negative γ_1 as that without homogeneous disorder but not for positive γ_1 . For $\hat{\alpha} = 2/\sqrt{3}$, there are still the modes locating in the imaginary frequency axis for negative γ_1 but not for positive γ_1 , for which new branch cuts emerge. These emerging modes in the high frequency region violate this correspondence.

- For large $\hat{\alpha}$ ($\hat{\alpha} = 2$), only for the dominate QNM, i.e., the ones closest to the real axis, the correspondence between the poles of $\text{Re}\sigma(\hat{\omega}; \gamma_1)$ and the ones of $\text{Re}\sigma_*(\hat{\omega}; -\gamma_1)$ approximately holds. As a whole, the pole structures for $\hat{\alpha} = 2$ are similar with that for $\hat{\alpha} = 2/\sqrt{3}$.

We also exhibit the QNMs for $\gamma_1 = -1$ with homogeneous disorder (the third columns in FIG.7, 8 and 9). When the homogeneous disorder is introduced, the new branch cuts attach to the imaginary frequency axis. Such pole structures are interesting and are worthy of further study such that we can understand the physics of these pole structures.

The dominant poles reveal the late time dynamics of the system. So, we shall study

the dominant pole behaviors such that we have a well understanding on the effect of the homogeneous disorder.

In our previous work [27], we have studied the conductivity at the low frequency in real axis for $\gamma_1 = -1$ with homogeneous disorder. For small $\hat{\alpha}$, it exhibits a sharp DS peak. Though it is not the Drude peak, we can phenomenologically describe this peak by the Drude formula (see FIG.5 in [27])

$$\sigma(\hat{\omega}) = \frac{K}{\Gamma - i\hat{\omega}}, \quad (21)$$

where Γ is the relaxation rate, which relates the relaxation time τ as $\Gamma = 1/\tau$. This peak in the real axis corresponds to a purely imaginary mode in complex frequency panel (see the left column in FIG.10). We also locate the position of the purely imaginary mode, which is listed in Table I. We find that the relaxation rates fitted by the Drude formula (21) are in very agreement with that by locating the position of the purely imaginary mode.

$\hat{\alpha}$	0	0.01	0.1	0.5
Γ_1	0.0114	0.0115	0.0120	0.0284
Γ_2	0.0114	0.0115	0.0122	0.0370

TABLE I: The relaxation rate Γ_i of the holographic system with $\gamma_1 = -1$ for different $\hat{\alpha}$. Γ_1 is fitted by the Drude formula (21) and Γ_2 is obtained by locating the position of the purely imaginary mode in complex frequency panel.

More detailed evolution of the dominant QNMs with $\hat{\alpha}$ for $\gamma_1 = -1$ is presented in FIG.10. Most of the dominant QNMs for the original theory, except for that approximately in the region of $\hat{\alpha} \in (1, 2/\sqrt{3})$, are the purely imaginary modes. Correspondingly, the dominant QNMs for the dual theory, except for that approximately in the region of $\hat{\alpha} \in (1, 2/\sqrt{3})$, are off axis.

Further, we study the evolution of the dominant QNMs with $\hat{\alpha}$ for $|\gamma_1| = 0.02$, which is shown in FIG.11. We describe the properties as what follows.

- For $\gamma_1 = -0.02$, all the dominant QNMs for the original theory are purely imaginary modes. With the increase of $\hat{\alpha}$, these modes firstly migrate downwards, and then migrate upwards, finally approaches to a certain value. The evolution of the dominant QNMs for the dual theory with $\gamma_1 = 0.02$ is similar with that for the original theory

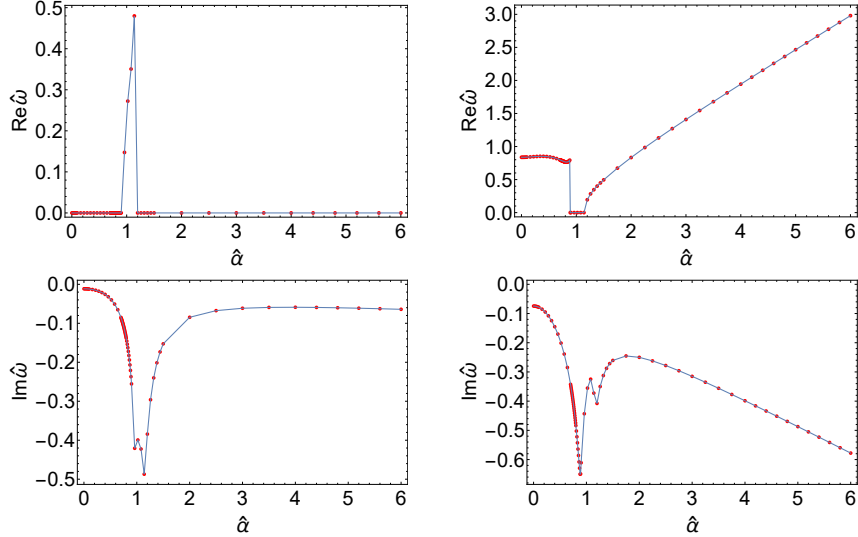


FIG. 10: Evolution of the dominant QNMs with $\hat{\alpha}$ for $\gamma_1 = -1$. The left column is the QNMs for the original theory, and the right one is that for its dual theory.

with $\gamma_1 = -0.02$. Such evolution is also similar with that for 4 derivative theory studied in [29]. As a whole, there is a qualitative correspondence between the evolution of the poles for the original theory for $\gamma_1 = -0.02$ and that for its dual theory for $\gamma_1 = 0.02$. But we would like to point out that as discussed above, for small $\hat{\alpha}$, the poles for the dual theory are closer to the real frequency axis than that for the original theory. In contrast, the correspondence hold more well for large $\hat{\alpha}$.

- For $\gamma_1 = 0.02$, the dominant poles for the original theory are off-axis for small $\hat{\alpha}$. With the increase of $\hat{\alpha}$, the poles migrate downwards and is closer to the real axis. When $\hat{\alpha}$ reaches the value of $\hat{\alpha} \simeq 0.8$, the poles merge into one purely imaginary pole. And then, when $\hat{\alpha}$ is beyond $\hat{\alpha} \simeq 1.4$, the purely imaginary pole splits into two off-axis modes. While for $\gamma_1 = -0.02$, the evolution of the dominant poles for the dual theory is similar with that for the original theory with $\gamma_1 = 0.02$. But when $\hat{\alpha} > 3.5$, the pole for the dual theory with $\gamma_1 = -0.02$ becomes a purely imaginary one.

V. CONCLUSION AND DISCUSSION

In this paper, we extend our previous work [27], which studied the optical conductivity from 6 derivative theory on top of EA-AdS geometry, to the holographic response of its EM

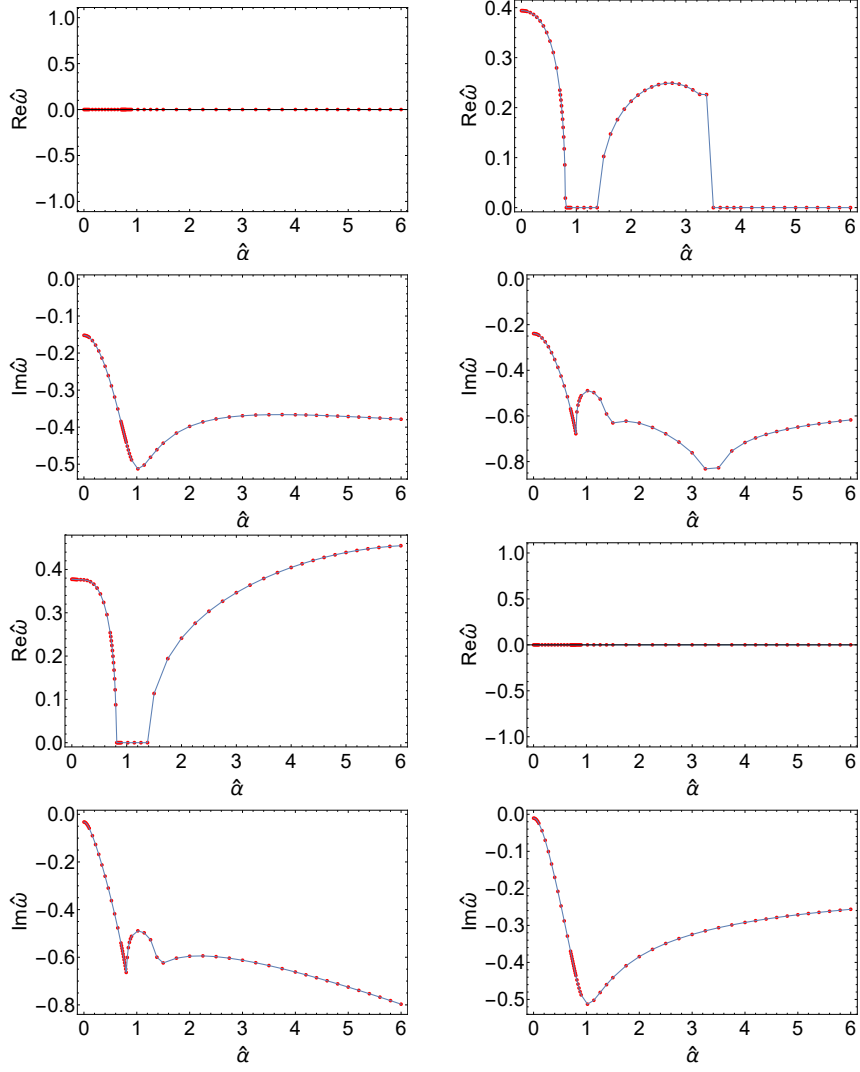


FIG. 11: Evolution of the dominant QNMs with $\hat{\alpha}$ for $|\gamma_1| = 0.02$ (the first two rows are for $\gamma_1 = -0.02$ and the last two rows for $\gamma_1 = 0.02$). The left columns are the QNMs for original theory, and the right ones are that for its dual theory.

dual theory. In particular, we explore thoroughly the EM duality. Also we study the QNMs and the EM duality in complex frequency panel.

In absence of the homogeneous disorder, with the change of the sign of γ_1 , the particle-vortex duality only holds for small $|\gamma_1|$. With the increase of $|\gamma_1|$, this duality violates. When the homogeneous disorder is introduced, as found in 4 derivative theory, we find that for the specific value of $\hat{\alpha} = 2/\sqrt{3}$, the optical conductivity of the original theory is almost the same as that of the dual one when the sign of γ_1 changes. For other value of $\hat{\alpha}$, the particle-vortex

also approximately holds with the change of the sign of γ_1 . Therefore, we can conclude that the homogeneous disorder make the pseudogap-like of the low frequency conductivity of the original theory becomes small dip, while suppresses the sharp peak of the EM dual theory such that we have an approximate particle-vortex duality with the change of the sign of γ_1 .

The properties of the QNMs are also analyzed. In absence of the homogeneous disorder, the qualitative correspondence between the poles of $\text{Re}\sigma(\hat{\omega}; \gamma_1)$ and the ones of $\text{Re}\sigma_*(\hat{\omega}; -\gamma_1)$ holds well at low frequency only for small γ_1 . When γ_1 becomes large, this correspondence is also violated even at the low frequency region. For $\gamma_1 = -1$, new branch cuts of QNMs are observed. When the homogeneous disorder is introduced and its strength is small, the approximate correspondence between the poles of $\text{Re}\sigma(\hat{\omega}; \gamma_1)$ and the ones of $\text{Re}\sigma_*(\hat{\omega}; -\gamma_1)$ recovers in low frequency region even for $|\gamma_1| = 0.02$. But in the high frequency region, this correspondence is violated. For large $\hat{\alpha}$, this correspondence is strongly violated and only holds for the dominate QNMs. For $\gamma_1 = -1$, the homogeneous disorder drives the off-axis new branch cuts for $\hat{\alpha} = 0$ to the purely imaginary modes.

The evolution of the dominant QNMs with $\hat{\alpha}$ are also explored. We find that all the dominant QNMs for the original theory with $\gamma_1 = -0.02$ and that for the dual theory with $\gamma_1 = 0.02$ are purely imaginary modes. Their evolutions are also similar. As a whole, there is a qualitative correspondence between them. However, for the evolution of the dominant QNMs for the original theory with $\gamma_1 = 0.02$ and that for the dual theory with $\gamma_1 = -0.02$, the case is somewhat different. The main difference is that the modes are not again the purely imaginary ones except for some specific $\hat{\alpha}$.

There are lots of open questions worthy of further study.

- We would like to carry out an analytical study on the complex frequency conductivity by matching method developed in [32]. Also we can analytically work out the QNMs by WKB method as [5, 8]. These analytical analysis can surely provide more physical insight and understanding into our present observation.
- At present, the perturbative black brane solution to the first order of the coupling parameter from 4 derivative theory has been worked out in [28, 33–39] and the related exploration, including holographic metal-insulator transition, holographic entanglement, holographic thermalization etc., at finite charge density on top of the perturbative background with HD correctons. In future, it is also interesting to further study the

QNMs, including scalar, vector and tensor modes, from HD theory at finite charge density⁵.

- The dispersing QNMs with finite momentum deserve further studying. It surely reveals richer physics of the system.
- The superconducting phase from HD theory has been widely explored in [40–49] and references therein. It is also interesting to study the QNMs in the superconducting phase of these models such that we can get richer insight and understanding on the HD theory.

Acknowledgments

This work is supported by the Natural Science Foundation of China under Grant No.11775036.

Appendix A: Brief analysis on the stability

In [27], by analyzing the instabilities of gauge mode and the causality in CFT, in addition to the constraint from $\text{Re}\sigma(\omega) \geq 0$, we confirm that the constraint $\gamma_1 \leq 1/48$, which has been obtained over SS-AdS geometry in [8], also holds over EA-AdS geometry. In this section, we further examine this constraint by studying the QNMs. Indeed, we find that when $\gamma_1 \leq 1/48$, all the QNMs are in the LHP.

First, it has been shown in FIG.10 and 11 that for $\gamma_1 = -1$, $|\gamma_1| = 0.02$ and $\hat{\alpha} \in [0, 6]$, all the poles and zeros, which are the poles of the dual theory, are in the LHP. In addition, we also see that when $\hat{\alpha} \rightarrow \infty$, the imaginary modes approach to a constant or even continue to migrate downwards. Therefore, we can conclude that for the selected γ_1 , the modes are stable for all $\hat{\alpha}$.

And then, for represent $\hat{\alpha}$, we show the poles and zeros for larger region of $\gamma_1 \leq 1/48$. As that on top of SS-AdS geometry in [8], the dominant poles from EA-AdS geometry are purely imaginary modes and also asymptotically approaches the real $\hat{\omega}$ -axis as $\gamma_1 \rightarrow -\infty$.

⁵ The QNMs of massless scalar field over the perturbative black hole with spherical symmetry horizon have been studied in [35].

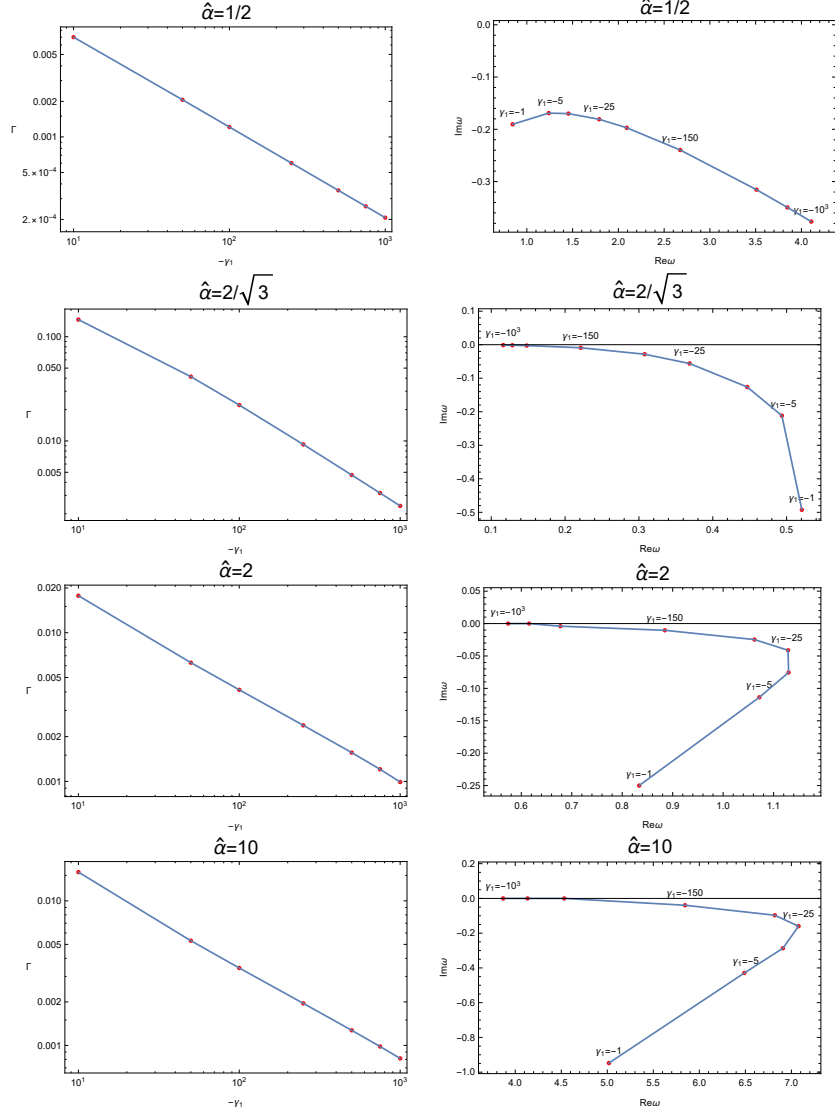


FIG. 12: Left plot: Location of the dominate QNM for different $\hat{\alpha}$. Red dots is the numerical data and the blue line is the power-law fit of the form $a/|\gamma_1|^b$. Right plot: Location of the next QNM closet to the real axis, a zero, for different $\hat{\alpha}$.

$\hat{\alpha}$	1/2	$2/\sqrt{3}$	2	10
a	0.040	0.957	0.076	0.072
b	0.761	0.816	0.632	0.662

TABLE II: The coefficients of the power-law fit of the form $a/|\gamma_1|^b$ for the dominant poles for different $\hat{\alpha}$.

In addition, the data can be well fitted by a power-law formula as $a/|\gamma_1|^b$. The coefficients a

and b are listed in Table II. We can see that at least over the 3 decades we have studied, the fit is very well as shown in FIG.12. We would like to point out that this result is consistent with that the peak of the conductivity at low frequency becomes sharper with the decrease of γ_1 and finally approaches a delta function as $\gamma_1 \rightarrow -\infty$. For the zeros, we also see that they all locate at the LHP at least over the 3 decades we have studied here (see right plots in FIG.12). Therefore, by the analysis of QNMs, we again confirm that the gauge mode is stable over EA-AdS geometry when the coupling parameter is confined to $\gamma_1 \leq 1/48$.

-
- [1] R. C. Myers, S. Sachdev and A. Singh, “Holographic Quantum Critical Transport without Self-Duality,” *Phys. Rev. D* **83**, 066017 (2011) [arXiv:1010.0443 [hep-th]].
 - [2] S. Sachdev, “What can gauge-gravity duality teach us about condensed matter physics?,” *Ann. Rev. Condensed Matter Phys.* **3**, 9 (2012) [arXiv:1108.1197 [cond-mat.str-el]].
 - [3] S. A. Hartnoll, A. Lucas and S. Sachdev, “Holographic quantum matter,” arXiv:1612.07324 [hep-th].
 - [4] A. Ritz and J. Ward, “Weyl corrections to holographic conductivity,” *Phys. Rev. D* **79**, 066003 (2009) [arXiv:0811.4195 [hep-th]].
 - [5] W. Witczak-Krempa and S. Sachdev, “The quasi-normal modes of quantum criticality,” *Phys. Rev. B* **86**, 235115 (2012) [arXiv:1210.4166 [cond-mat.str-el]].
 - [6] W. Witczak-Krempa and S. Sachdev, “Dispersing quasinormal modes in 2+1 dimensional conformal field theories,” *Phys. Rev. B* **87**, 155149 (2013) [arXiv:1302.0847 [cond-mat.str-el]].
 - [7] W. Witczak-Krempa, E. S. Sørensen and S. Sachdev, “The dynamics of quantum criticality via Quantum Monte Carlo and holography,” *Nature Phys.* **10**, 361 (2014) [arXiv:1309.2941 [cond-mat.str-el]].
 - [8] W. Witczak-Krempa, “Quantum critical charge response from higher derivatives in holography,” *Phys. Rev. B* **89**, no. 16, 161114 (2014) [arXiv:1312.3334 [cond-mat.str-el]].
 - [9] E. Katz, S. Sachdev, E. S. Sørensen and W. Witczak-Krempa, “Conformal field theories at nonzero temperature: Operator product expansions, Monte Carlo, and holography,” *Phys. Rev. B* **90**, no. 24, 245109 (2014) [arXiv:1409.3841 [cond-mat.str-el]].
 - [10] S. Bai and D. W. Pang, “Holographic charge transport in 2+1 dimensions at finite N ,” *Int. J. Mod. Phys. A* **29**, 1450061 (2014) [arXiv:1312.3351 [hep-th]].

- [11] R. C. Myers, T. Sierens and W. Witczak-Krempa, “A Holographic Model for Quantum Critical Responses,” *JHEP* **1605**, 073 (2016) Addendum: [*JHEP* **1609**, 066 (2016)] [arXiv:1602.05599 [hep-th]].
- [12] A. Lucas, T. Sierens and W. Witczak-Krempa, “Quantum critical response: from conformal perturbation theory to holography,” *JHEP* **1707**, 149 (2017) [arXiv:1704.05461 [hep-th]].
- [13] J. P. Wu, “Holographic quantum critical conductivity from higher derivative electrodynamics,” *Phys. Lett. B* **785**, 296 (2018).
- [14] K. Damle and S. Sachdev, “Nonzero-temperature transport near quantum critical points,” *Phys. Rev. B* **56**, no. 14, 8714 (1997) [cond-mat/9705206 [cond-mat.str-el]].
- [15] T. Andrade and B. Withers, “A simple holographic model of momentum relaxation,” *JHEP* **1405**, 101 (2014) [arXiv:1311.5157 [hep-th]].
- [16] A. Donos and S. A. Hartnoll, “Interaction-driven localization in holography,” *Nature Phys.* **9**, 649 (2013) [arXiv:1212.2998].
- [17] A. Donos and J. P. Gauntlett, “Holographic Q-lattices,” *JHEP* **1404**, 040 (2014) [arXiv:1311.3292 [hep-th]].
- [18] A. Donos and J. P. Gauntlett, “Novel metals and insulators from holography,” *JHEP* **1406**, 007 (2014) [arXiv:1401.5077 [hep-th]].
- [19] D. Vegh, “Holography without translational symmetry,” arXiv:1301.0537 [hep-th].
- [20] M. Blake and D. Tong, “Universal Resistivity from Holographic Massive Gravity,” *Phys. Rev. D* **88**, no. 10, 106004 (2013) [arXiv:1308.4970 [hep-th]].
- [21] S. Grozdanov, A. Lucas, S. Sachdev and K. Schalm, “Absence of disorder-driven metal-insulator transitions in simple holographic models,” *Phys. Rev. Lett.* **115**, no. 22, 221601 (2015) [arXiv:1507.00003 [hep-th]].
- [22] Y. Ling, P. Liu, C. Niu and J. P. Wu, “Building a doped Mott system by holography,” *Phys. Rev. D* **92**, no. 8, 086003 (2015) [arXiv:1507.02514 [hep-th]].
- [23] Y. Ling, P. Liu and J. P. Wu, “A novel insulator by holographic Q-lattices,” *JHEP* **1602**, 075 (2016) [arXiv:1510.05456 [hep-th]].
- [24] X. M. Kuang and J. P. Wu, “Thermal transport and quasi-normal modes in Gauss-CBonnet-axions theory,” *Phys. Lett. B* **770**, 117 (2017) [arXiv:1702.01490 [hep-th]].
- [25] X. M. Kuang, J. P. Wu and Z. Zhou, “Holographic transports from Born-Infeld electrodynamics with momentum dissipation,” arXiv:1805.07904 [hep-th].

- [26] J. P. Wu, X. M. Kuang, G. Fu, “Momentum dissipation and holographic transport without self-duality,” *Eur. Phys. J. C* **78**, no. 8, 616 (2018) [arXiv:1609.04729 [hep-th]].
- [27] G. Fu, J. P. Wu, B. Xu and J. Liu, “Holographic response from higher derivatives with homogeneous disorder,” *Phys. Lett. B* **769**, 569 (2017) [arXiv:1705.06672 [hep-th]].
- [28] J. P. Wu, “Transport phenomena and Weyl correction in effective holographic theory of momentum dissipation,” *Eur. Phys. J. C* **78**, no. 4, 292 (2018).
- [29] J. P. Wu and P. Liu, “Quasi-normal modes of holographic system with Weyl correction and momentum dissipation,” *Phys. Lett. B* **780**, 616 (2018) [arXiv:1804.10897 [hep-th]].
- [30] C. P. Herzog, P. Kovtun, S. Sachdev and D. T. Son, “Quantum critical transport, duality, and M-theory,” *Phys. Rev. D* **75**, 085020 (2007) [hep-th/0701036].
- [31] A. Jansen, “Overdamped modes in Schwarzschild-de Sitter and a Mathematica package for the numerical computation of quasinormal modes,” *Eur. Phys. J. Plus* **132**, no. 12, 546 (2017) [arXiv:1709.09178 [gr-qc]].
- [32] T. Faulkner, H. Liu, J. McGreevy and D. Vegh, “Emergent quantum criticality, Fermi surfaces, and AdS(2),” *Phys. Rev. D* **83**, 125002 (2011) [arXiv:0907.2694 [hep-th]].
- [33] Y. Ling, P. Liu, J. P. Wu and Z. Zhou, “Holographic Metal-Insulator Transition in Higher Derivative Gravity,” *Phys. Lett. B* **766**, 41 (2017) [arXiv:1606.07866 [hep-th]].
- [34] W. J. Li, P. Liu and J. P. Wu, “Weyl corrections to diffusion and chaos in holography,” *JHEP* **1804**, 115 (2018) [arXiv:1710.07896 [hep-th]].
- [35] S. Mahapatra, “Thermodynamics, Phase Transition and Quasinormal modes with Weyl corrections,” *JHEP* **1604**, 142 (2016) [arXiv:1602.03007 [hep-th]].
- [36] A. Dey, S. Mahapatra and T. Sarkar, “Thermodynamics and Entanglement Entropy with Weyl Corrections,” *Phys. Rev. D* **94**, no. 2, 026006 (2016) [arXiv:1512.07117 [hep-th]].
- [37] A. Dey, S. Mahapatra and T. Sarkar, “Holographic Thermalization with Weyl Corrections,” *JHEP* **1601**, 088 (2016) [arXiv:1510.00232 [hep-th]].
- [38] A. Mokhtari, S. A. Hosseini Mansoori and K. Bitaghsir Fadafan, “Diffusivities bounds in the presence of Weyl corrections,” arXiv:1710.03738 [hep-th].
- [39] J. P. Wu, B. Xu and G. Fu, “Holographic fermionic spectrum with Weyl correction,” arXiv:1802.09027 [hep-th].
- [40] J. P. Wu, Y. Cao, X. M. Kuang and W. J. Li, “The 3+1 holographic superconductor with Weyl corrections,” *Phys. Lett. B* **697**, 153 (2011) [arXiv:1010.1929 [hep-th]].

- [41] D. Z. Ma, Y. Cao and J. P. Wu, “The Stuckelberg holographic superconductors with Weyl corrections,” *Phys. Lett. B* **704**, 604 (2011) [arXiv:1201.2486 [hep-th]].
- [42] J. P. Wu and P. Liu, “Holographic superconductivity from higher derivative theory,” *Phys. Lett. B* **774**, 527 (2017) [arXiv:1710.07971 [hep-th]].
- [43] Y. Ling and X. Zheng, “Holographic superconductor with momentum relaxation and Weyl correction,” *Nucl. Phys. B* **917**, 1 (2017) [arXiv:1609.09717 [hep-th]].
- [44] D. Momeni and M. R. Setare, “A note on holographic superconductors with Weyl Corrections,” *Mod. Phys. Lett. A* **26**, 2889 (2011) [arXiv:1106.0431 [physics.gen-ph]].
- [45] D. Momeni, N. Majd and R. Myrzakulov, “p-wave holographic superconductors with Weyl corrections,” *Europhys. Lett.* **97**, 61001 (2012) [arXiv:1204.1246 [hep-th]].
- [46] Z. Zhao, Q. Pan and J. Jing, “Holographic insulator/superconductor phase transition with Weyl corrections,” *Phys. Lett. B* **719**, 440 (2013) [arXiv:1212.3062].
- [47] D. Momeni, R. Myrzakulov and M. Raza, “Holographic superconductors with Weyl Corrections via gauge/gravity duality,” *Int. J. Mod. Phys. A* **28**, 1350096 (2013) [arXiv:1307.8348 [hep-th]].
- [48] D. Momeni, M. Raza and R. Myrzakulov, “Holographic superconductors with Weyl corrections,” *Int. J. Geom. Meth. Mod. Phys.* **13**, 1550131 (2016) [arXiv:1410.8379 [hep-th]].
- [49] L. Zhang, Q. Pan and J. Jing, “Holographic p-wave superconductor models with Weyl corrections,” *Phys. Lett. B* **743**, 104 (2015) [arXiv:1502.05635 [hep-th]].
- [50] S. A. H. Mansoori, B. Mirza, A. Mokhtari, F. L. Dezaki and Z. Sherkatghanad, “Weyl holographic superconductor in the Lifshitz black hole background,” *JHEP* **1607**, 111 (2016) [arXiv:1602.07245 [hep-th]].